# The Rate of Single Event Upsets in Electronic Circuits onboard Spacecraft

## N. V. Kuznetsov

*Skobeltsyn Institute of Nuclear Physics, Moscow State University, Vorob'evy gory, Moscow, 119899 Russia*
Received March 23, 2004

**Abstract**—Models and methods in use for quantitative estimates of the occurrence of single event upsets in microchips of orbiting spacecraft are considered. A calculation and experimental technique for determining the rate of these effects is described, taking into account spatial and temporal distributions of the fluxes of high-energy particles in the space and their penetration through protective shields. Examples of its application for the orbit of the *International Space Station* are presented.

## INTRODUCTION

For the first time a communication about random changes in information codes (at a single bit level) of a semiconductor RAM of control units of a geosynchronous satellite was published in 1975 [1]. It was suggested that the effect could be explained by the influence of separate heavy charged particles (HCP) of galactic cosmic rays (GCR) which penetrated into memory cells of the RAM. It was referred to as soft errors and later as single event upsets (SEU) of the logical state of memory cells or single failures (in Russian literature). At the present time, the effect of SEU occurrence in memory cells of RAM onboard spacecraft is confirmed by numerous flight experiments. The list of the best known such experiments [2–17] is given in the Table.

In several years after discovering SEU in memory microchips onboard spacecraft, the SEU effect associated with the influence of separate HCP was observed in RAM microchips of the dynamic memory [18]. It was found that in this case SEU were induced by alpha-particles of radioactive isotopes contained in the substance of microchip packages. After that the SEU effect began to be extensively studied at accelerators of heavy ions and protons [19] and also with the use of radio isotopic and laser sources [20]. Due to these studies, various types of single event effects (SEE) are established and under investigation [21] which violate normal functioning of very large scale integration circuits (VLSIC). From the physical point of view SEE are explained by the fact of appearance in the active regions of VLSIC (having micron and submicron size) of non-equilibrium charge carriers from the track of a single high-energy particle, which results in the following phenomena.

—Pulses of photocurrent in a semiconductor structure lead to inversion of the logical state of memory cells or to a functional interruption of VLSIC operation.

—Breakdowns of p-n junctions result in latching up (thyristor effect) of CMOS structures or in burning out of power MOS transistors.

—Breakdowns of the gate dielectric or variations of built-in charge in MOS transistors cause sticking (parametric failure) of separate elements of VLSIC.

Space vehicles (instrumentation modules) used for studying single event inversions of memory cells of RAM VLSIC

| Spacecraft | Country of instrumentation design | References |
|---|---|---|
| *TDRS-1* | USA | [2, 3] |
| *LEASAT-1, -2, -3* | USA | [4] |
| *CRRES* | USA | [5, 6] |
| *SAMPEX* | USA | [3] |
| *APEX* | USA | [7] |
| *UoSAT-2, -3, -5* | UK | [8] |
| *S80/T* | UK | [9] |
| *KITSAT-1* | UK | [9] |
| *SPOT-1, -2, -3* | France | [10] |
| *EXOS-D* | Japan | [11] |
| *MOS-1* | Japan | [12] |
| *ETS-V* | Japan | [12] |
| *ETS-VI* | Japan | [12] |
| *ADEOS* | Japan | [12] |
| *Meteor-3* (TOMS) | USA | [3] |
| *Mir* (EXEQ) | France | [13] |
| *ELEKTRO-1* | Russia | [14] |
| *INTERBALL-2* | Russia | [15] |
| *MPTB* | USA | [16] |
| *SAC-C* (ICARE) | France | [17] |

The above effects become a cause of appearance of both intermittent failures (malfunctions) and permanent failures of VLSIC in electronic systems of control, and systems of data acquisition and storage onboard spacecraft. There are different circuit-analysis, algorithmic, and program methods in order to minimize such failures and to exclude their influence when functional tasks are executed. The optimal choice of these methods is based not only on knowing the nature of SEE and the causes of their occurrence, but also on quantitative estimates of their rate in VLSIC due to irradiation by the fluxes of space radiation particles. Therefore, in order to provide for capacity of the spacecraft electronics for work, special methods of predicting SEE in VLSIC during spacecraft flights are developed. These methods use the models of occurrence of SEE in VLSIC and models of the fluxes of high-energy particles in space, taking into account their penetration through the spacecraft shield.

Accounting for the complexity of contemporary models, the most rational solution to this problem is constructed on the basis of their computerized versions. For example, this principle is used in widely known American (CREME96[1]) and European (SPENVIS[2]) information systems.

The aim of this paper is to discuss general principles and basic features of the method that is developed in Skobeltsyn Institute of Nuclear Physics of Moscow State University in order to estimate and predict SEE in VLSIC onboard spacecraft.

## 1. GENERAL STATEMENTS AND FORMULAS

The rate of SEE, $\nu$, is the quantity which characterizes the level of occurrence of SEE in VLSIC. It is equal to the mean (over a preset time interval) number of SEE appearing in VLSIC per unit time. Taking into account that the degree of danger (for VLSIC functioning) is different for different types of SEE and that different methods should be used for protection of instrumentation against their influence, the values of $\nu$ for VLSIC in spacecraft devices must be determined separately for each type of SEE. In doing so, one should take into account that this quantity in calculations of the rate of SEE of any type is a sum of two components

$$\nu = \nu_{ion} + \nu_p, \quad (1)$$

where $\nu_{ion}$ is the rate of SEE appearing as a result of direct penetration of HCP of the space radiation into VLSIC (direct mechanism of SEE origination); and $\nu_p$ is the rate of SEE appearing as a result of production of residual nuclei and recoil nuclei in VLSIC through nuclear interactions of cosmic ray protons with the matter of VLSIC chips (nuclear mechanism of SEE origination).

[1] http://crsp3.nrl.navy.mil./creme96
[2] http://www.spenvis.oma.be/spenvis

For evaluation of the SEE rate $\nu_{ion}$ under the action of HCP flux the value $L$ of linear energy transfer (LET) of an HCP to the VLSIC substance is chosen as an energy characteristic of the particle, and the value of $\nu_{ion}$ is determined using the following formula:

$$\nu_{ion} = \iiint \sigma_{ion}(L, \theta, \varphi)F(L, x)dLd(\cos\theta)d\varphi, \quad (2)$$

where $F(L, x)$ is the differential spectrum of linear energy transfer (LET) of a directed flux of isotropic HCP $[(\text{s cm}^2 \text{ sr MeV}/(\text{g/cm}^2))^{-1}]$ incident onto the VLSIC surface after their passage through a shield with thickness $x$, and $\sigma_{ion}(L, \theta, \varphi)$ is the cross section of SEE in the plane perpendicular to the direction of HCP incidence (this cross section depends on LET $L$ of an HCP and on the angles of HCP incidence onto the VLSIC surface, polar angle $\theta$ and azimuth $\varphi$).

The SEE rate $\nu_p$ under the action of the flux of protons is calculated with the help of the following multiple integral:

$$\nu_p = \iiint \sigma_p(E, \theta, \varphi)F_p(E, x)dEd(\cos\theta)d\varphi, \quad (3)$$

where $F_p(E, x)$ is the differential energy spectrum of direction isotropic flux of protons $[(\text{s cm}^2 \text{ sr MeV})^{-1}]$ incident on VLSIC after having passed through a shield with thickness $x$, and $\sigma_p(E, \theta, \varphi)$ is the cross section of SEE perpendicular to the direction of proton incidence (depends on proton energy $E$ and on the angles of incidence of protons onto the VLSIC surface, polar angle $\theta$ and azimuth $\varphi$). It should be emphasized that in formulas (2) and (3) the flux of particles incident onto the VLSIC surface is assumed to be isotropic. This assumption is the only possible when calculations are performed, since it is in agreement with a similar assumption made in the models of particles in space. In these models the fluxes of particles arriving to spacecraft from different directions are averaged. The same assumption remains to be valid if the fluxes of particles which penetrated inside the spacecraft are calculated for the center of a spherical shield with a constant thickness of its envelope.

Thus, in order to calculate the SEE rate in VLSIC according to formulas (2) and (3) one needs to know the following.

(1) The differential energy spectrum of directed flux of protons $F_p(E, x)$ and differential LET spectrum of directed HCP flux $F(L, x)$ incident on VLSIC.

(2) Numerical functions of SEE cross sections $\sigma_{ion}(L, \theta, \varphi)$ and $\sigma_p(E, \theta, \varphi)$ which are individual characteristics of VLSIC and are responsible for its radiation resistance (sensitivity, failure- and fault-tolerance) with respect to occurrence of a particular type of SEE.

## 2. FLUXES OF PARTICLES OF SPACE RADIATION

Determination of the energy and LET spectra of particles appearing in formulas (2) and (3) is made in two stages.

At the first stage, computer versions of the models of particle fluxes in the near-terrestrial space are used:

—the model of proton fluxes in the Earth's radiation belts (ERB) which uses the data "flux–geomagnetic coordinates" of model AP8 [22];

—the dynamical model of galactic cosmic rays (GCR) [23] which establishes the fluxes of protons and nuclei of various chemical elements in GCR outside the Earth's magnetosphere;

—the probabilistic model of solar cosmic rays (SCR) [24] which predicts the total and peak fluxes of protons and ions in SCR for a preset probability of their appearance beyond the Earth's magnetosphere.

Conversion of model energy spectra of the fluxes of ERB protons to a given orbit is performed taking into account the interrelation of geocentric and geomagnetic coordinates established by the model of the Earth's magnetic field [25], including the secular drift of its inner sources [26]. The energy spectra of GCR and SCR particle fluxes in spacecraft orbits crossing the magnetosphere are found from model energy spectra of the fluxes of these particles taking their cutoff by the Earth's magnetosphere. The last procedure uses the tables of vertical cutoff rigidities [27] for undisturbed magnetosphere converted to the coordinates of a given orbit with corrections for local time and the level of disturbance of the Earth's magnetic field [28]. All procedures of coordinate conversion are performed with the help of computer codes simulating the trajectory of spacecraft motion along the orbit. At various points of spacecraft trajectory the differential energy spectra of particle fluxes are calculated step by step during several days of spacecraft flight. Finally, the averaged and peak (maximally possible) spectra of particle fluxes in orbit are found.

At the second stage, radiation conditions behind the spacecraft shield are calculated. To this end, the energy spectra in orbit are transformed into energy spectra of the fluxes of protons (and neutrons generated in the shield) and into LET spectra of HCP. The spectra are calculated that should originate in the center of a spherical shield with a mass thickness of 0.01 to 100 $g/cm^2$. These transformations are carried out using specially developed approximating expressions that generalize numerical data on particle energy losses in the shield matter [29], and also using the fluxes of secondary protons and neutrons due to nuclear interactions of the protons from ambient space with the spacecraft shield matter [30].

Some examples of differential energy spectra of protons and of LET protons of HCP for various spacecraft orbits can be found in [31].

## 3. CROSS SECTION OF SINGLE EVENT EFFECTS

### 3.1. The Impact of HCP

In the developed procedure the numerical function $\sigma_{ion}(L, \theta, \varphi)$ characterizing the sensitivity of VLSIC to SEE occurrence is established based on the experimental data that are obtained at heavy ion accelerators and interpreted using the model of a "thin sensitive layer" [32]. According to this model, function $\sigma_{ion}(L, \theta, \varphi)$ in formula (2) for arbitrary azimuth angle $\varphi$ (asymmetry in azimuth is assumed) is written in the form

$$\sigma_{ion}(L, \theta, \varphi) = \sigma^{(exp)}(L_{ef})\cos\theta, \qquad (4)$$

where $L_{ef} = L/\cos\theta$ are the effective values of LET, and one-variable function $\sigma^{(exp)}(L_{ef})$ is invariant with respect to any angle of particle incidence onto the VLSIC surface.

The method of experimental determination of numerical values of the SEE cross section and the form of function $\sigma^{(exp)}(L_{ef})$ are discussed[3] in many papers (see, for example, [33]). It was found that the values of $\sigma^{(exp)}(L_{ef})$ for different VLSIC and for different types of SEE increased and tended to saturation with increasing $L_{ef}$.

As an example, Fig. 1 presents the experimental values of $\sigma^{(exp)}(L_{ef})$ obtained for the SEU effect after testing two RAM VLSIC [34, 35]. The same figure presents the curves approximating the experimental data with the use of a two-parameter function of the following form [36, 37]

$$\sigma(L_{ef}) = \sigma_0'\exp\left(-\frac{U}{L/\cos\theta}\right). \qquad (5)$$

Function (5) is used in the developed method for approximation of the experimental data $\sigma^{(exp)}(L_{ef})$. As was shown by analysis [37], in accuracy (necessary for practical applications) this function is a little inferior to four-parameter Weibull function [33] widely used in world practice. At the same time, it allows one to use the existing databases[4] which include only two basic parameters of VLSIC sensitivity: experimental cross section of saturation, $\sigma_0 = \sigma(L_{ef} \longrightarrow \infty)$, and experimental value of the LET threshold, $L_c = L(\sigma \longrightarrow 0)$. The relationship of these two basic parameters with the parameters of function (5) is established in [37]: $\sigma_0' = \sigma_0$ and $U \cong 10L_c$.

The model of a "thin sensitive layer" is experimentally confirmed for many VLSIC manufactured using the planar technology, as well as invariance of function $\sigma(L_{ef})$ with respect to the angle of incidence on the

---

[3] When studying the effect of SEU in RAM VLSIC the values of $\sigma^{(exp)}(L_{ef})/B_0$ (with dimensionality [$cm^2$/bit]) are often used instead of the values of $\sigma^{(exp)}(L_{ef})$ characterizing the sensitivity of the entire VLSIC (where $B_0$ is the memory capacity of VLSIC)

[4] For example, http://Radnet.jpl.nas.gov or http://radhome.gsfc.nasa.gov.
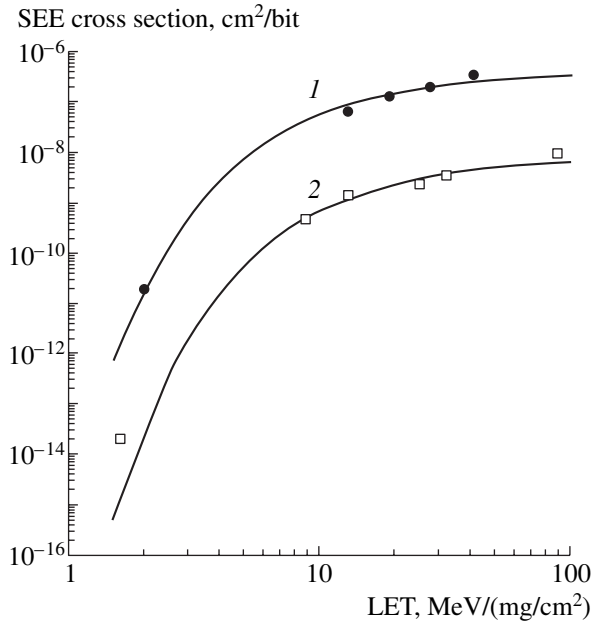
SEE cross section, cm$^2$/bit



**Fig. 1.** Cross sections for single event inversions of the logical state of memory cells in RAM VLSIC Hitachi HM628128 (*1*) and IBM0165400 (*2*) versus LET of heavy ions. Points represent experimental data [38, 39] and curves are the approximations of experimental data by formula (8).

VLSIC surface θ. At the same time, some authors refined expression (4) in order to find the function $\sigma_{ion}(L, \theta, \varphi)$ having in mind the finite thickness of sensitive layer $z_0$ [38] or the dependence of the SEE cross section on azimuth angle [39]. In addition, it has been found in [40] that for modern VLSIC of dynamic memory with super-large degree of integration (more than 4M) significant deviations from the law $\sigma_{ion}(L, \theta, \varphi) = \sigma(L_{ef})\cos\theta$ may take place. This is explained by the fact that in VLSIC of dynamic memory, which are manufactured based on the trench technology, sensitive volumes have comparable dimensions in all directions $\{x_0, y_0\} \cong z_0$. In this case, the model of "isotropic cross section" [40] is more suitable for describing the angular dependence of SEE cross section (if one also neglects the azimuth dependence) assuming $\sigma_{ion}(L, \theta, \varphi) \cong \sigma(L)$.

Taking the said above into account, in the method discussed, when the SEE rate is calculated for VLSIC in spacecraft orbits (formula (2)), in addition to the relation $\sigma_{ion}(L, \theta, \varphi) = \sigma(L_{ef})\cos\theta$ assumed for the model of "thin sensitive layer" the approximation $\sigma_{ion}(L, \theta, \varphi) = \sigma(L)$ is used for VLSIC of dynamic memory with super-large degree of integration.

### 3.2. Impact of Protons

Under proton impact, it is a priori assumed that the SEE cross section $\sigma_p(E, \theta, \varphi)$ does not depend on the angles of incidence onto the VLSIC surface, i.e., $\sigma_p(E, \theta, \varphi) \equiv \sigma_p(E)$. From the physical standpoint this means

that the concept of secondary HCP (residual nuclei and recoil nuclei) produced as a result of nuclear interactions in VLSIC matter remains the same independent of the direction of proton motion, as well as the distribution of energy released by them in the sensitive volume. In the general case, such a dependence exists [41, 42], but it is assumed to be negligible for all practical purposes when the SEE rate under the action of space radiation is predicted.

Numerical values of $\sigma_p(E)$ for VLSIC can be found in two ways. The first method is to determine the values of $\sigma_p(E)$ experimentally at accelerators with variation of proton energy ($E > 10$ MeV), and then to approximate these values using a two-parameter Bendel function [43].

The second method consists in using the experimental function of SEE cross section $\sigma_{ion}(L, \theta, \varphi)$ under the action of HCP (this function was considered above) and nuclear data on spatial and energy characteristics of secondary HCP produced in VLSIC under irradiation by protons. This method is preferable from both physical and practical points of view. Owing to it, one can save time and costs for testing VLSIC at unique accelerator facilities. In addition, one can reduce the number of problems which emerge unavoidably when the results for VLSIC tested at different accelerators are coordinated.

The second way of determining the numerical values of $\sigma_p(E)$ requires that complex computer programs be developed (for example, [44–47]), and its is used in the method of predicting the SEE rate described in this paper. In this case, the calculation is performed using the following formula

$$\sigma_p(E) = n_a S_V Z_V \sum_j \iiint \frac{\sigma(\varepsilon)}{S_V} \qquad (6)$$
$$\times \omega_j(E, E', \theta', \varphi') dE' d(\cos\theta') d\varphi'.$$

where $n_a$ is the concentration of atoms in VLSIC matter, $S_V$ and $Z_V$ are, respectively, the cross section and depth of the volume in which HCP are produced, $\sigma(\varepsilon)$ is the SEE cross section for HCP releasing energy $\varepsilon$ in the sensitive volume $V_0$, and $\omega_j(E, E', \Omega') = [d^2\sigma_j^{(нис)}(E)/dE'd\Omega']$ is doubly differential cross section of production of secondary HCP of the type $j$ (with mass number $A$ and charge $Z$) with energy $E'$ and the direction of motion $\Omega' \equiv \Omega(\theta', \varphi')$ which characterizes the collision of protons of energy $E$ with nuclei of the VLSIC matter. Summation in formula (6) is made over HCP of different types and integration is made over their energy $E'$ and two angles ($\theta'$ and $\varphi'$).

The calculation according to formula (6) was made using the Monte Carlo method simulating in each event the point of HCP production in the volume $V = S_V \times Z_V$ and the type of HCP and its spatial and energy characteristics (energy $E'$ and motion direction $\Omega(\theta', \varphi')$).
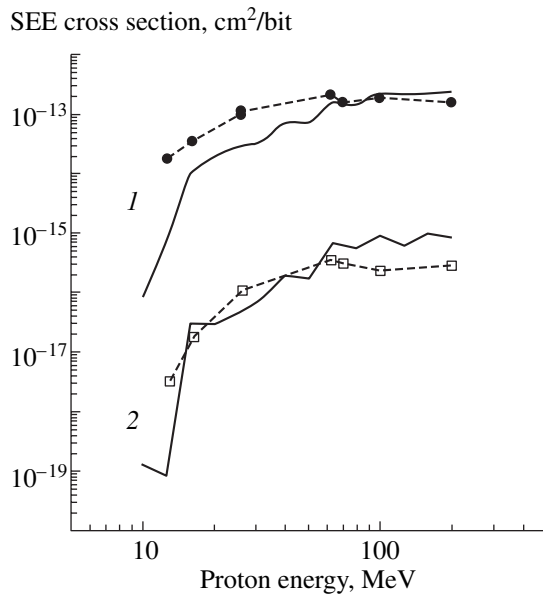
SEE cross section, cm$^2$/bit



**Fig. 2.** Cross sections for single event inversions of the logical state of memory cells in RAM VLSIC Hitachi HM628128 (*1*) and IBM0165400 (*2*) versus proton energy. Points and dashed curves represent experimental data [57] and solid curves are the data of calculation according to the procedure described in the text.

SEE rate, s$^{-1}$



**Fig. 3.** Mean (*1, 2, 3*) and maximum (*1', 2', 3'*) calculated rate of single event inversions in RAM VLSIC IBM0165400 in the *ISS* orbit (the year of minimum solar activity) versus the thickness of a shield of spherical form under the action of the fluxes of (*1, 1'*) ERB protons; (*2, 2'*) GCR protons and HCP; and (*3, 3'*) protons and HCP of SCR which can appear with a probability of 50%.

The latter characteristics are chosen in accordance with their distribution which is established by the function $\omega_j(E, E', \Omega')$. The form and numerical values of this function for protons in the interval of proton energies from 10 MeV to 10 GeV are found in advance for each residual nucleus of the type *j* (including alpha-particles and recoil nuclei) using nuclear data on cross sections of inelastic (and quasi-elastic) nuclear collisions of protons with silicon nuclei [48–52] and accounting for available information [52–54] about the kinematics of decay of a nucleus which gained a momentum from a projectile particle.

Further, in each event the energy $\varepsilon$ released by HCP is found taking into account their energy losses [29] within rectangular sensitive volume $V_0 = \sigma_0 z_0$, where $\sigma_0(<S_V)$ and $z_0(<Z_V)$ are the cross section of SEE saturation (for the sensitive volume) and the depth of the sensitive volume, respectively, determined for the VLSIC under investigation at an accelerator of heavy ions (see above). Knowing the released energy $\varepsilon$, the value of $\sigma(\varepsilon)$ is determined from the experimental function of HCP SEE cross section $\sigma(L_{ef})$ (Fig. 1) for the VLSIC under study, provided that $L_{ef} = \varepsilon/z_0$.

Figure 2 presents calculated functions $\sigma_p(E)$ for RAM VLSIC whose SEE cross section under the action of HCP is shown in Fig. 1. Figure 2 also presents the experimental data for $\sigma_p(E)$ known from the results of testing VLSIC of the same type at proton accelerators [55]. One can see that there is a certain discrepancy
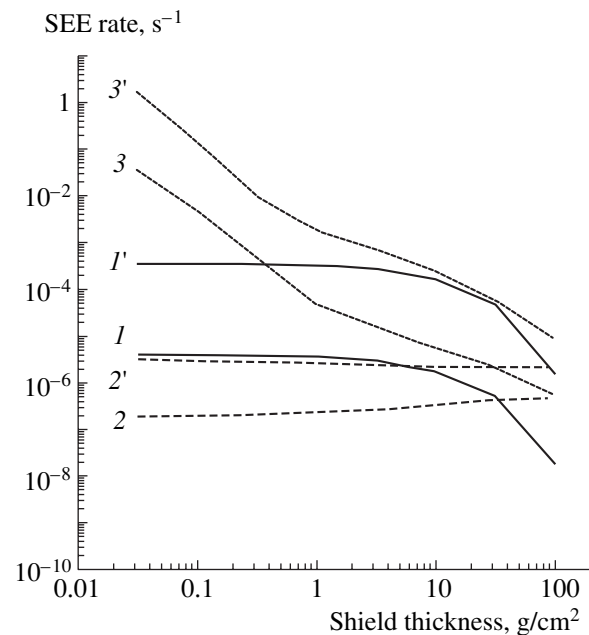
between calculated and experimental values of $\sigma_p(E)$. However, as was shown by the analysis, it lies within the usual scatter of experimental values of $\sigma_p(E)$ which is observed in various experiments for VLSIC of one and the same type.

## 4. RESULTS OF EVALUATION OF SEE RATE

The choice and procedures of determination of integrand functions in formulas (2) and (3) that are considered in two preceding sections allow us to make an evaluation of SEE rate $\nu$ for VLSIC onboard spacecraft taking into account the radiation conditions in orbits and the effective thickness of a protective shield around the VLSIC. The specially developed software [31] also allows the variations of quantity $\nu$ to be modeled along the flight trajectory of a spacecraft depending on its time of flight. This makes it possible to make differential analysis of VLSIC serviceability on separate segments of the spacecraft trajectory. The output calculation data which can be obtained using the developed procedure and software are presented in Figs. 3 and 4.

Figure 3 shows a set of calculation data that allows one for a given time period and specified orbit

—to compare the SEE rate under the action of particle fluxes of each radiation field separately;

—to determine the mean and maximum possible values of the SEE rate which occur in a spacecraft orbit,
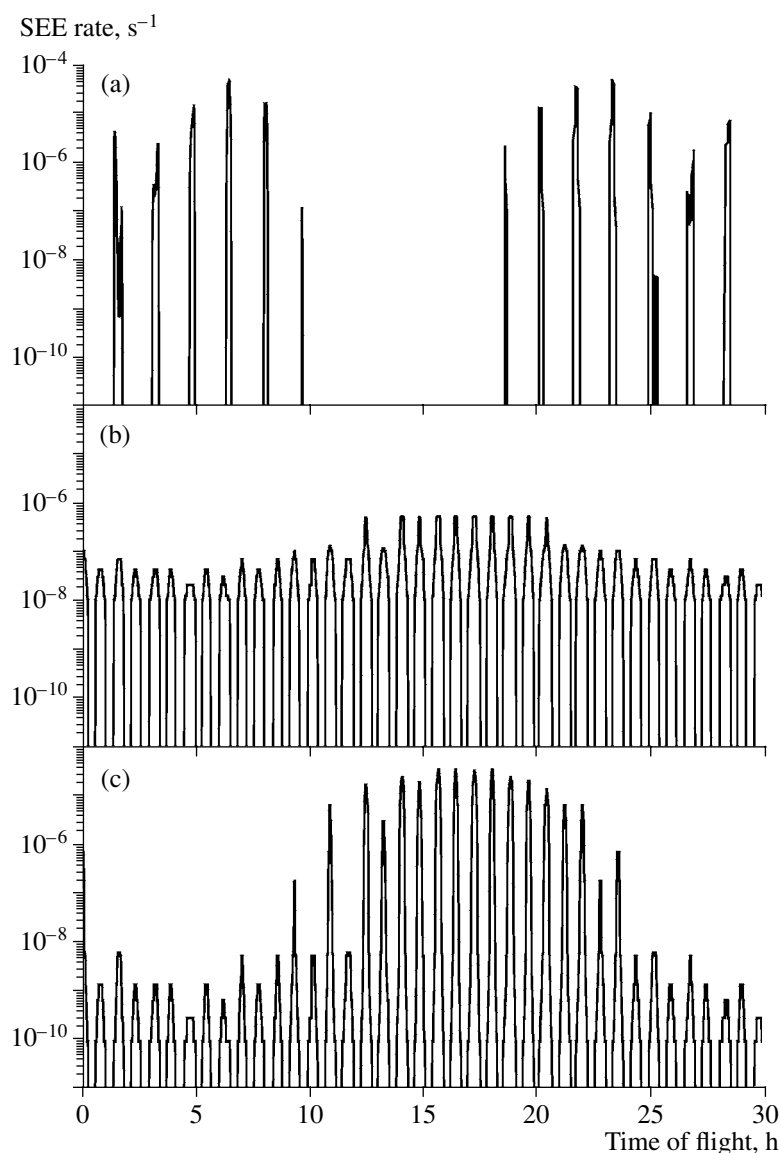
**Fig. 4.** Calculated rate of single events inversions in RAM VLSIC Hitachi HM628128 in the *ISS* orbit as a function of time of the station flight under the action of the fluxes of (a) ERB protons, (b) GCR protons and HCP, and (c) protons and HCP of a super-strong SCR event (similar to the November 2000 event). The thickness of a spherical shield is 1 g/cm$^2$.

including the effects made by the fluxes of SCR particles;

—to evaluate the changes in the SEE rate that take place when the thickness of a shield surrounding VLSIC is varied.

For example, one can see from the results of calculations of the SEU rate for logical states of VLSIC memory cells of dynamical RAM IBM0165400 (the SEU cross sections for this VLSIC are presented in Figs. 1 and 2) shown in Fig. 3 for the *ISS* orbit that the peak fluxes of SCR particles may constitute the most serious hazard for VLSIC. These fluxes appear in very strong SCR events (similar to those recorded in November 2002 or in November 2003). However, the probability of occurrence of such events is small, which

is reflected in the fact that the mean SEE rate calculated for SCR particle fluxes is substantially lower. In the absence of SCR events, as is seen in Fig. 3, the main source of failures in the *ISS* orbit is the fluxes of ERB protons. The significant difference between mean and maximum values of the SEU rate due to ERB protons indicates to strong variations of the fluxes of ERB protons along the *ISS* orbit. Indeed, it is well known that the proton fluxes at the *ISS* orbit strongly increase in the region of the South Atlantic Anomaly (SAA). At a shield thickness of more than ~50 g/cm$^2$ the fluxes of GCR particles give a certain contribution to the mean SEU rate in the *ISS* orbit. In this case, the SEU rate due to GCR particle fluxes slightly increases with the shield thickness. This effect is explained by a contribution to

the SEU rate of secondary protons produced behind the shield as a result of nuclear interactions of GCR protons with the shield matter.

The results of more detailed calculations which allow one to study the SEE rate variations as a function of time of *ISS* flight along the orbit are presented in Fig. 4. This figure shows the cyclograms of SEU rate values for VLSIC HM628128 (SEU cross sections are presented in Figs. 1 and 2) behind a spherical shield 1 g/cm² thick under the action of particle fluxes of ERB, GCR, and an extremely strong SCR event (similar to the event of November 2000). No allowance was made in the calculations for disturbance of the magnetosphere. An analysis of the data presented in Fig. 4 shows that the SEU rate caused by the action of the fluxes of ERB protons (Fig. 4a) sharply increases on separate orbit segments located in the SAA region. There is also a prolonged period of the flight time (~8–10 h per day) when no SEU occur, since in this period the orbit does not cross the SAA region, and there are virtually no fluxes of ERB protons. In this period only the fluxes of GCR particles (Fig. 4b) and the particle fluxes of the SCR event (Fig. 4c) are the cause of SEU occurrence. One should also emphasize that the maximum SEU rate $\nu_{max}^{(ERB)}$ due to the irradiation by ERB protons is comparable to the maximum SEU rate $\nu_{max}^{(SCR)}$ due to the action of particle fluxes from a very strong SCR event. The values of $\nu_{max}^{(GCR)}$ due to the effect of the GCR particle fluxes are two–three orders of magnitude lower that the values of $\nu_{max}^{(ERB)}$.

## CONCLUSION

In conclusion, let us summarize basic features of the considered method (and software), which was developed to evaluate and predict SEE onboard spacecraft.

—Up-to-date models of ERB, GCR, and SCR particle fluxes are used taking into account their variations depending on spacecraft coordinates in the near-Earth space, solar activity, local time, and planetary disturbances of the Earth's magnetic field.

—Variations of particle fluxes along the spacecraft trajectory are calculated taking into account their transformations (including the appearance of additional fluxes of secondary neutrons and protons) behind protective shields with thickness of 0.01 to 100 g/cm².

—The mean and extreme values of SEE rate are determined for a specified time of spacecraft flight.

—The SEE rate under the action of the fluxes of both protons and HCP of radiation fields in space is determined for VLSIC using the data of testing the VLSIC under study at accelerators of heavy ions.

## REFERENCES

1. Binder, D., Smith, E.C., and Holman, A.B., Satellite Anomalies from Galactic Cosmic Rays, *IEEE Trans. Nucl. Sci.*, 1975, vol. 22, no. 6, pp. 2675–2680.

2. Wilkinson, D.C., Daughtridge, S.C., Stone, J.L., *et al.*, TDRS-1 Single Event Upsets and Effects of the Space Environment, *IEEE Trans. Nucl. Sci.*, 1991, vol. 38, no. 6, pp. 1708–1714.

3. Seidleck, C.M., LaBel, K.A., Moran, A.K., *et al.*, Single Event Effect Flight Data Analysis of Multiple NASA Spacecraft and Experiments; Implications to Spacecraft Electrical Designs, *Proc. of RADECS-95 (Sept. 18–22, 1995, Arcachon, France)*, pp. 581–588.

4. Shoga, M., Adams, P., Chenette, D.L., *et al.*, Verification of Single Event Upset Rate Estimation Methods with On-Orbit Observations, *IEEE Trans. Nucl. Sci.*, 1987, vol. 34, no. 6, pp. 1256–1261.

5. Campbell, A., McDonald, P., and Ray, K., Single Event Upset Rates in Space, *IEEE Trans. Nucl. Sci.*, 1992, vol. 39, no. 6, pp. 1828–1835.

6. Weatherford, T.R., McDonald, P.T., Campbell, A.B., and Langworthy, J.B., SEU Rate Prediction and Measurement of GaAs SRAMs onboard the *CRRES* Satellite, *IEEE Trans. Nucl. Sci.*, 1993, vol. 40, no. 6, pp. 1463–11470.

7. Adolphsen, J., Barth, J.J., Stassinopoulos, E.G., *et al.*, Single Event Upset Rates on 1 Mbit and 256 Kbit Memories: CRUX Experiment on APEX, *IEEE Trans. Nucl. Sci.*, 1995, vol. 42, no. 6, pp. 1964–1974.

8. Underwood, C.I., The Single-Event-Effect Behavior of Commercial-Off-The-Shelf Memory Devices—A Decade in Low-Earth Orbit, *Proceedings of RADECS-97 (Sept. 15–19, 1997, Cannes, France)*, pp. 251–258.

9. Underwood, C.I. and Oldfield, M.K., Observed Radiation-Induced Degradation of Commercial-Off-The-Shelf (COTS) Devices Operating in Low-Earth Orbit, *IEEE Trans. Nucl. Sci.*, 1998, vol. 45, no. 6, pp. 2737–2744.

10. Ecoffet, R., Prieur, M., Del Castillo, M.F., *et al.*, Influence of Solar Cycle on SPOT-1, -2, -3 Upset Rates, *IEEE Trans. Nucl. Sci.*, 1995, vol. 42, no. 6, pp. 1983–1987.

11. Takagi, Sh., Nakamura, T., Kohno, T., *et al.*, Observation of Radiation Environment with EXOS-D, *IEEE Trans. Nucl. Sci.*, 1993, vol. 40, no. 6, pp. 1491–1497.

12. Coka, T., Matsumoto, H., and Nemoto, N., SEE Flight Data from Japanese Satellites, *IEEE Trans. Nucl. Sci.*, 1998, vol. 45, no. 6, pp. 2771–2778.

13. Falguere, D., Duzellier, S., and Ecoffet, R., SEE In-Flight Measurement on the *MIR* Orbital Station, *IEEE Trans. Nucl. Sci.*, 1994, vol. 41, no. 6, pp. 2346–2350.

14. Kuznetsov, N.V., Mishin, G., Khodnenko, V.P., and Shatskii, M.V., Estimation of Single Event Upsets in Onboard Instrumentation of Geosynchronous *ELEK-TRO* Spacecraft, in *Radiatsionnaya stoikost' elektron-*

*nykh sistem. "Stoikost'-99". Vyp. 2* (Radiation Tolerance of Electronic Systems: "Tolerance-99", no. 2), Moscow: SPELS, 1999, pp. 23–24.

15. Chesalin, L., Ryazanova, E., and Lakutina, E., Localization of Onboard Processor Upsets in the Magnetosphere and Their Automatic Correction on the *INTERBALL-2 (Auroral Probe)* Satellite, *Kosm. Issled.*, 1999, vol. 37, no. 6, pp. 567–572.

16. Barak, J., Single Event Upsets in the Dual-Port-Board SRAMs of the MPTB Experiment, *Proc. of RADECS-99*, 2000, pp. 582–587.

17. Falguere, D., Bosher, D., Nuns, T., *et al.*, In-Flight Observations of the Radiative Environment and Its Effects on Devices in the SAC-C Polar Orbit, *IEEE Trans. Nucl. Sci.*, 2002, vol. 49, no. 6, pp. 2782–2787.

18. May, T.C. and Woods, M.H., Alpha-Particle-Induced Soft Error in Dynamic Memories, *IEEE Trans. Electron Devices*, 1979, vol. ED-26, no. 1, pp. 29–33.

19. Koga, R., Single-Event Effect Ground Test Issues, *IEEE Trans. Nucl. Sci.*, 1996, vol. 43, no. 3, pp. 661–670.

20. Buchner, S., McMorrow, D., Melinger, J., and Campbell, A.B., Laboratory Tests for Single-Event Effects, *IEEE Trans. Nucl. Sci.*, 1996, vol. 43, no. 2, pp. 678–686.

21. Sexton, F.W., Measurement of Single Event Phenomena in Devices and IC's, *IEEE NSREC Short Course*, 1992.

22. Sawyer, D.M. and Vette, J.I., *AP-8 Trapped Environment for Solar Maximum and Solar Minimum*, Greenbelt, MD: National Space Science Data Center, 1976 (NSSDC 76-06).

23. Nymmik, R.A., Panasyuk, M.I., and Suslov, A.A., Galactic Cosmic Ray Flux Simulation and Prediction, *Adv. Space Res.*, 1995, vol. 17, no. 2, pp. 19–22.

24. Nymmik, R.A., Probabilistic Model for Fluences and Peak Fluxes of Solar Energetic Particles, *Rad. Meas.*, 1999, vol. 30, pp. 287–296.

25. Tsyganenko, N.A., A Magnetosphere Magnetic Field Model with a Warped Tail Current Sheet, *Planet. Space Sci.*, 1989, vol. 37, pp. 5–20.

26. Heynderickx, D., Comparison between Methods to Compensate for the Secular Motion of the South Atlantic Anomaly, *Rad. Meas.*, 1996, vol. 26, pp. 325–331.

27. Shea, M.A. and Smart, D.F., A World Grid of Calculated Cosmic Ray Vertical Cutoff Rigidities for 1980, *Proc. 25th ICRC*, 1997, vol. 3, pp. 415–417.

28. Nymmik, R.A., The Problems of Cosmic Ray Particle Simulation for the Near-Earth Orbital and Interplanetary Flight Conditions, *Rad. Meas.*, 1999, vol. 30, p. 8.

29. Ziegler, J.F., Biersack, J.P., and Littmark, U., *The Stopping and Range of Ions in Solids*, New York: Pergamon, 1985.

30. Dementyev, A. and Sobolevsky, N., SHIELD—Universal Monte Carlo Hadron Transport Code: Scope and Applications, *Rad. Meas.*, 1999, vol. 30, pp. 553–557.

31. Kuznetsov, N.V. and Panasyuk, M.I., Cosmic Radiation and Prediction of Upset- and Fault-Tolerance of Integrated Circuits in Onboard Instrumentation of Spacecraft, *Voprosy Atomnoi Nauki i Tekhniki (VANT), Ser. Radiats. Vozd. na Elektr. Apparat.*, 2001, nos. 1–2, pp. 3–8.

32. Binder, D., Analytic SEU Rate Calculation Compared to Space Data, *IEEE Trans. Nucl. Sci.*, 1988, vol. 35, no. 6, pp. 1570–1574.

33. Petersen, E., Cross Section Measurement and Upset Rate Calculations, *IEEE Trans. Nucl. Sci.,* 1996, vol. 43, no. 6, pp. 2805–2813.

34. Harboe-Sorensen, R., Daly, E.J., Adams, L., *et al.*, Observation and Prediction of SEU in Hitachi SRAMs in Low Altitude Polar Orbits, *IEEE Trans. Nucl. Sci.*, 1993, vol. 40, no. 6, pp. 1498–1504.

35. Fox, A.J., Abare, W.E., and Ross, A., Suitability of COTS IBM 64M DRAM in Space, *Proc. of RADECS-97 (Sept. 15–19, 1997, Cannes, France)*, pp. 240–244.

36. Edmonds, L.D., SEU Cross Sections Derived from a Diffusion Analysis, *IEEE Trans. Nucl. Sci.*, 1996, vol. 43, no. 6, pp. 3207–3217.

37. Kuznetsov, N.V., Mishin, G.A., and Khodnenko, V.P., Two-Parameter Approximation of Experimental Dependence of Cross Section for Upsets in RAM Chips on Linear Energy Transfer of Heavy Ions, *Voprosy Atomnoi Nauki i Tekhniki (VANT), Ser. Radiats. Vozd. na Elektr. Apparat.*, 2001, nos. 1–2, pp. 9–12.

38. Petersen, E.I., Pickel, J.C., Smith, E.C., *et al.*, Geometrical Factors in SEE Rate Calculations, *IEEE Trans. Nucl. Sci.*, 1993, vol. 40, no. 6, pp. 1888–1908.

39. Reed, R.A., McNulty, P.J., Beauvais, W.J., and Roth, D.R., Charge Collection Spectroscopy, *IEEE Trans. Nucl. Sci.*, 1993, vol. 40, no. 6, pp. 1880–1887.

40. Guertin, S.M., Edmonds, L.D., and Swift, M., Angular Dependence of DRAM Upset Susceptibility and Implications for Testing and Analysis, *IEEE Trans. Nucl. Sci.*, 2000, vol. 47, no. 6, pp. 2380–2385.

41. Reed, R.A., McNulty, P.J., and Abdel-Kader, W.G., Implications of Angle of Incidence in SEU Testing of Modern Circuits, *IEEE Trans. Nucl. Sci.*, 1994, vol. 41, no. 6, pp. 2049–2054.

42. Levinson, J., Barak, J., Zentner, A., *et al.*, Angular Dependence of Proton Induced Events and Charge Collection, *IEEE Trans. Nucl. Sci.*, 1994, vol. 41, no. 6, pp. 2098–2102.

43. Stapor, W.J., Meyers, J.P., Langworthy, J.B., and Petersen, E.L., Two Parameter Bendel Model Calculations for Predicting Proton Induced Upset, *IEEE Trans. Nucl. Sci.*, 1990, vol. 37, no. 6, pp. 1966–1973.

44. McNulty, P.J., Abdel-Kader, W.G., and Bisgrove, J.M., Methods for Calculating SEU Rates for Bipolar and NMOS Circuits, *IEEE Trans. Nucl. Sci.*, 1985, vol. 32, no. 6, pp. 41980–41984.

45. Doucin, B., Patin, Y., Lochard, J.P., *et al.*, Characterization of Proton Interactions in Electronic Components, *Proc. of RADECS-93 (Sept. 13–16, 1993, Saint Malo, France)*, 1994, pp. 532–539.

46. Miroshkin, V.V. and Tverskoy, M.G., Two Parameter Model for Predicting SEU Rate, *IEEE Trans. Nucl. Sci.*, 1994, vol. 41, no. 6, pp. 2085–2092.

47. Barak, J., Analytical Microdosimetry Model for Proton-Induced SEU in Modern Devices, *IEEE Trans. Nucl. Sci.*, 2001, vol. 48, no. 6, pp. 1937–1945.

48. Barashenkov, V.S. and Toneev, V.P., *Vzaimodeistviya vysokoenergeticheskikh chastits i atomnykh yader s yadrami* (Interaction of High-Energy Particles and Atomic Nuclei with Nuclei), Moscow: Atomizdat, 1972.

49. Silberberg, R. and Tsao, C.H., Partial Cross-Sections in High-Energy Nuclear Reactions and Astrophysical Applications. I. Targets with Z < 28, *The Astrophys. J. Suppl. Ser.,* 1973, vol. 25, no. 220(1), pp. 315–333.

50. Grutter, A., Excitation Functions for Radioactive Isotopes Produced by Proton Bombardment of Cu and Al in the Energy Range of 16 to 70 MeV, *Nucl. Phys. A,* 1982, vol. A383, pp. 98–108.

51. Denisov, F.P. and Mekhedov, V.N., *Yadernye reaktsii pri vysokikh energiyakh* (High-Energy Nuclear Reactions), Moscow: Atomizdat, 1972.

52. Westfall, G.D., Sextro, R.G., Poskanzer, A.M., *et al.*, Energy Spectra of Nuclear Fragments Produced by High Energy Protons, *Phys. Rev. C*, 1978, vol. 17, no. 4, pp. 1368–1381.

53. Wilson, J.W., Townsend, L.W., Naely, J.E., *et al., BRYN-TRN: A Baryon Transport Model, NASA TP-2887,* 1989.

54. Greiner, D.E., Lindstrom, P.J., Heckman, H.H., *et al.*, Momentum Distributions of Isotopes Produced by Fragmentation of Relativistic $^{12}$C and $^{16}$O Projectiles, *Phys. Rev. Lett.*, 1975, vol. 35, no. 3, pp. 152–155.

55. Duzellier, S., Ecoffet, R., Falguere, D., *et al.*, Low Energy Proton Induced SEE Memories, *IEEE Trans. Nucl. Sci.*, 1997, vol. 44, no. 6, pp. 2306–2310.